




Cite this: *New J. Chem.*, 2019, 43, 16915

Simple fabrication of a carbaldehyde based fluorescent “turn-on” probe for the selective and sole detection of Pd²⁺: application as test strips†

Chandan Kumar Manna, Saswati Gharami, Krishnendu Aich, Lakshman Patra and Tapan K. Mondal *

A new fluorescent “turn-on” probe (DHMC) has been designed and synthesized to selectively detect Pd²⁺ among other cations at physiological pH. Upon incremental addition of Pd²⁺ into the probe solution, a “turn-on” emission enhancement was noticed with a ~69 nm red shift at 562 nm in CH₃CN/H₂O (4/1, v/v) solution. The limit of detection and binding constant values have been determined and found to be on the order of 7.4×10^{-8} M and 1.7×10^5 M⁻¹ respectively, which clearly suggests that the probe is very efficient in detecting Pd²⁺ at very minute levels and also the DHMC–Pd²⁺ complexation is stable enough too. A brilliant application of the probe has been explored which indicates that DHMC can detect Pd²⁺ in the solid state too. DFT and TDDFT calculations are carried out to interpret the electronic structure and sensing mechanism.

Received 20th August 2019,
Accepted 26th September 2019

DOI: 10.1039/c9nj04313f

rsc.li/njc

Introduction

Palladium is a platinum group element and one of the most valuable transition metals. It is extensively used in a range of applications such as the jewelry business, coating materials, dental crowns and chemical catalysts.^{1–4} Mainly, Pd-catalyzed C–C cross-coupling reactions have been renowned as competent and handy tools for the synthesis of organic compounds including pharmaceutical products.^{5,6} However, an adverse influence of this metal on human health has created a grave concern as palladium ions can bind to thiol-containing proteins (*e.g.* casein and silk fibroin), DNA or other biomolecules because of their high nucleophilicity.^{7,8} Palladium residues in pharmaceutical compounds or in the environment may cause a substantial hazard especially for environmental pollution emissions to water and soil.⁹ Therefore, the governmental regulation on the proposed maximum nutritional intake of palladium is less than 1.5–15 µg per person per day.¹⁰ Therefore, design and development of a selective and sensitive analytical method for the recognition of palladium in the environment is essential to assess possible adverse health effects caused by this particular metal residue.

The conventional techniques used for quantification of palladium species, such as atomic absorption spectroscopy

(AAS), inductively coupled plasma atomic emission spectroscopy, solid-phase micro extraction high-performance liquid chromatography *etc.*, frequently proved to be more time-consuming, and they often demand complicated sample preparation and also they are more expensive and sophisticated and thus are not so appropriate for real-time and *in situ* analysis.¹¹ So currently the fabrication of fluorescent molecular probes is among the most cultivated techniques owing to their simplicity of application in solution as well as their high sensitivity and selectivity and tunability for trace analytes.¹² As a result, the requirement of the development of this type of new fluorescent probes has become a vital area of research nowadays.¹³ Although there have been some reports on Pd²⁺ sensors recently,¹⁴ our probe still shows a simple synthetic route and distinguishes Pd²⁺ solely among other cations in acetonitrile–water medium (4/1, v/v).

So herein we have presented the design and development of a new fluorescent probe based on the carbaldehyde moiety which distinctly senses Pd²⁺ among other metal ions, displaying a high detection limit value of 7.4×10^{-8} M.

Experimental

Materials and methods

2-Amino-4-methylphenol was purchased from Aldrich. All the other organic materials and solvents were purchased from commercial sources and used without further purification. ¹H and ¹³C NMR spectra were recorded on a Bruker 300 MHz

Department of Chemistry, Jadavpur University, Kolkata – 700032, India.

E-mail: tapank.mondal@jadavpuruniversity.in

† Electronic supplementary information (ESI) available: NMR and MS of all new compounds, limit of detection determination, quantum yield calculation. CCDC 1939357. For ESI and crystallographic data in CIF or other electronic format see DOI: 10.1039/c9nj04313f

instrument. Electronic spectra were taken on a PerkinElmer Lambda 750 spectrophotometer. The fluorescence properties were measured using a Shimadzu RF-6000 fluorescence spectrophotometer at room temperature (298 K). HRMS mass spectra were recorded on a Waters (Xevo G2 Q-TOF) mass spectrometer. Lifetime decay studies were performed using a time-resolved spectrofluorometer from IBH, UK.

UV-vis method

For UV-vis titrations, a stock solution of the probe DHMC (10 μM) was prepared in $[(\text{CH}_3\text{CN}/\text{H}_2\text{O}), 4/1, \text{v/v}]$ (at 25 $^\circ\text{C}$) using HEPES buffered solution. The solutions of all the guest cations were prepared in deionized water using their chloride salts (1×10^{-5} M) using HEPES buffer at pH = 7.2. Solutions of an array of concentrations containing the probe and all the cations were prepared separately. The spectra of these solutions were recorded by means of the UV-vis method.

Fluorescence method

For emission titrations, the stock solution of the probe DHMC (10 μM) used was the same as that used for the UV-vis titration. Solutions of the guest cations (10^{-5} M) in deionized water were prepared following the similar procedure as mentioned in UV-vis experiment. Solutions of varieties of concentrations containing the probe and cations were prepared separately. The spectra of these solutions were recorded by means of the fluorescence method.

Synthesis of 7-diethylamino-3-[[[(2-hydroxy-5-methyl-phenylimino)-methyl]-chromen-2-one] (DHMC)

7-Diethylamino-2-oxo-2H-chromene-3-carbaldehyde (**1**) (0.30 g, 1.22 mmol) and 2-amino-4-methyl-phenol (**2**) (0.15 g, 1.22 mmol) were dissolved in 25 mL of acetonitrile. The reaction mixture was stirred at room temperature for about 4 h. After completion of the reaction, the solvent was removed under reduced pressure. The crude product was dissolved in a minimum volume of dichloromethane and subjected to column chromatography. The desired red band of DHMC was eluted using a 30% (v/v) ethyl acetate-petroleum ether mixture. On removal of the solvent under reduced pressure DHMC was obtained as a red solid, which was further dried under a vacuum. The yield was 0.360 g, 84%.

^1H NMR (300 MHz, CDCl_3): δ 8.90 (1H, s), 8.46 (1H, s), 7.42 (1H, d, $J = 8.8$), 7.16 (1H, s), 6.97 (1H, d, $J = 7.9$), 6.88 (1H, d, $J = 8.07$), 6.64 (1H, d, $J = 6.66$), 6.51 (1H, s), 3.45 (4H, q, $J = 6.9$), 2.29 (3H, s), 1.24 (6H, t, $J = 6.97$).

^{13}C NMR (75 MHz, CDCl_3): δ 12.6, 20.9, 35.4, 97.5, 108.4, 110.1, 110.3, 114.5, 114.9, 115.4, 116.8, 117.7, 119.8, 129.7, 132.6, 145.5, 151.4, 153.6, 157.8, 162.3, 188.1.

HRMS: calculated for $\text{C}_{21}\text{H}_{23}\text{N}_2\text{O}_3$ $[\text{M} + \text{H}]^+$ (m/z) = 351.1709; found = 351.1652.

Synthesis of the Pd^{2+} complex (DHMC- Pd^{2+}) of the probe

77 mg of DHMC was dissolved in 10 mL of methanol. 10 mL of a methanolic solution of Na_2PdCl_4 (65 mg) was added dropwise to the DHMC solution under stirring conditions. The stirring was continued further for 4 h at room temperature to yield a

deep red solution. DHMC- Pd^{2+} was collected by evaporation of the solvent under reduced pressure.

HRMS (ESI, positive): calcd for $\text{C}_{21}\text{H}_{21}\text{N}_2\text{O}_3\text{Pd}$ $[\text{M}]^+$ (m/z): 455.0587; found: 455.0356.

Theoretical study

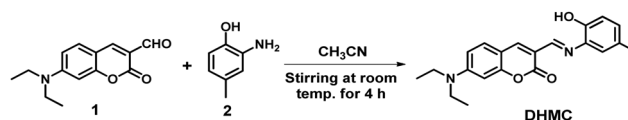
All calculations were done with the Gaussian 09 program package.¹⁵ Full geometry optimizations were executed with the help of the density functional theory (DFT) method at the B3LYP¹⁶ level for both the probe and the complex. The calculations were supported by the GaussView visualization program. All elements except palladium were assigned the 6-31+G(d) basis set. For the palladium atom the LanL2DZ basis with effective core potentials was employed.¹⁷ Vibrational frequency calculations were performed to be certain that the optimized geometries correspond to local minima and there were only positive eigenvalues. Vertical electronic excitations based on the B3LYP optimized geometries were calculated using the time-dependent density functional theory (TDDFT) formalism¹⁸ in acetonitrile using the conductor-like polarizable continuum model (CPCM).¹⁹

Results and discussion

The synthetic route towards the probe DHMC is shown in Scheme 1. Compound **1** was synthesized as reported in the literature.²⁰ The chemical structure of DHMC is confirmed by ^1H and ^{13}C NMR spectroscopy and ESI mass spectrometry (Fig. S1–S4, ESI[†]). Further it was affirmed by single crystal X-ray studies. Normal stirring of compound **1** and compound **2** in acetonitrile at room temperature for about 4 hours results in the desired “turn-on” fluorescent probe DHMC with a good yield of 84%.

Cation sensing properties

UV-vis study. The absorption spectral experiment of DHMC was performed using a $\text{CH}_3\text{CN}/\text{H}_2\text{O}$ (4/1, v/v) solution at 25 $^\circ\text{C}$ under physiological pH (10 mM HEPES buffer, pH = 7.2). The UV-vis spectrum of DHMC (10 μM) in $\text{CH}_3\text{CN}/\text{H}_2\text{O}$ (4/1, v/v) shows a moderately strong absorbance peak at 450 nm. But after gradual addition of Pd^{2+} into the solution of DHMC, a new absorbance peak at 496 nm appears with a shoulder peak at 462 nm and another one at 386 nm (Fig. 1) with a naked eye color change of yellow to pink, thus indicating the fact that Pd^{2+} is coordinated to the probe. A distinct isosbestic point was observed at 472 nm. The UV spectral pattern change may be attributed to the ICT process. Now to establish the selectivity of the probe (DHMC) further, the absorption spectral changes of DHMC were studied in the presence of other metal cations such



Scheme 1 Synthetic scheme of the probe, DHMC.

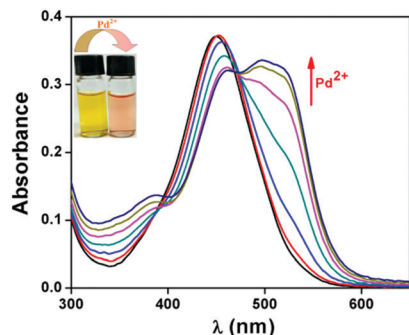


Fig. 1 Change in the UV-vis spectrum of DHMC (10 μM) upon addition of Pd^{2+} (0–15 μM) in $\text{CH}_3\text{CN}/\text{H}_2\text{O}$ (4/1, v/v). (The inset shows the change in the colour of DHMC from yellow to pink in ambient light.)

as Na^+ , K^+ , Ca^{2+} , Mg^{2+} , Mn^{2+} , Al^{3+} , Fe^{3+} , Cr^{3+} , Co^{2+} , Ni^{2+} , Hg^{2+} , Zn^{2+} , Cu^{2+} , Pb^{2+} and Cd^{2+} . No such absorbance change was observed for any other metals except for Al^{3+} and Fe^{3+} (Fig. S5, ESI †).

Emission study. The emission study was carried out in $\text{CH}_3\text{CN}/\text{H}_2\text{O}$ (4/1, v/v) solvent using HEPES buffer (10 mM) at physiological pH. A weak emission maximum at 493 nm ($\lambda_{\text{excitation}}$, 460 nm) was observed for solely the probe DHMC in $\text{CH}_3\text{CN}/\text{H}_2\text{O}$ (4/1, v/v) solvent. Now on incremental addition of Pd^{2+} to the DHMC solution, the emission maximum experiences a red shift of about 69 nm and the new emission maximum appears at 562 nm with a shoulder at 600 nm with a “turn-on” emission enhancement pattern (Fig. 2). This “turn-on” emission property may take place due to the ICT process that takes place in the probe after complexation.

The sensing ability of DHMC was also studied in the presence of other different metal ions such as K^+ , Ca^{2+} , Mg^{2+} , Mn^{2+} , Fe^{3+} , Cr^{3+} , Al^{3+} , Co^{2+} , Ni^{2+} , Hg^{2+} , Zn^{2+} , Cu^{2+} , Pb^{2+} and Cd^{2+} to reveal that the probe DHMC displays a “turn-on” response distinctly and solely towards Pd^{2+} in $\text{CH}_3\text{CN}/\text{H}_2\text{O}$ (4/1, v/v). No other metal ions show any changes as significant as those of Pd^{2+} (Fig. S6, ESI †).

The mole ratio plot drawn on the basis of the emission titration curve signifies that the probe DHMC shows an increase in emission intensity until DHMC: Pd^{2+} reaches ~ 1 . But after that there is no noticeable change in the emission

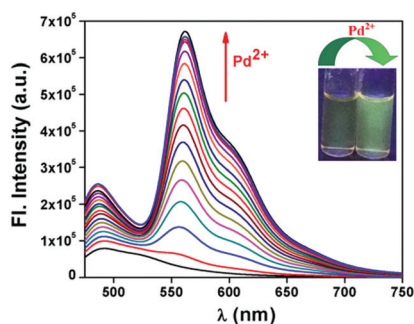


Fig. 2 Change in the emission spectra of DHMC (10 μM) upon gradual addition of Pd^{2+} (0–15 μM) in $\text{CH}_3\text{CN}/\text{H}_2\text{O}$ (4/1, v/v) (HEPES buffer, pH = 7.2). (The inset shows the change in colour of DHMC from colorless to green in a UV-chamber.)

intensity. Now to assess the stoichiometry of the complex of DHMC with Pd^{2+} , a Job's plot experiment was executed. The maximum shows the mole fraction at 0.5 for Pd^{2+} , which corresponds to the 1:1 complex formation of DHMC and Pd^{2+} (Fig. S7, ESI †). Now the detection limit of DHMC for Pd^{2+} was calculated to be 7.41×10^{-8} M, which was determined from the fluorescence spectral change of DHMC following the equation $\text{LOD} = K \times \text{SD}/S$, where ‘SD’ is the standard deviation of the blank solution of the probe and ‘S’ is the slope of the curve (Fig. S8, ESI †). Now the emission intensity of DHMC increased linearly at 562 nm with the amount of Pd^{2+} added in between 0 and 14.5 μM ($R^2 = 0.9909$) (Fig. S9, ESI †). The low limit of detection clearly suggests that DHMC is highly efficient in detecting Pd^{2+} even in very minute amounts. Furthermore, the association constant (K_a) of DHMC for Pd^{2+} was also determined using the Benesi–Hildebrand equation and was found to be 1.69×10^5 M^{-1} (Fig. S10, ESI †), which establishes the fact that the formation of DHMC– Pd^{2+} is stable enough.

We have also studied the lifetime decay profile of the free probe (DHMC) and in the presence of Pd^{2+} to understand the excited state stability. Here, the fluorescence lifetime of the free probe (DHMC) is significantly enhanced in the presence of Pd^{2+} . The lifetimes of DHMC and the DHMC– Pd^{2+} complex are found to be 0.54 ns and 3.16 ns, respectively, and fitted well with a bi-exponential decay (Fig. S11, ESI †).

After that, we have executed a competitive experiment on DHMC by measuring its emission intensity in the presence of other metal ions (20 μM) in order to study the precise emissive response of DHMC. It is noted from the experiment that the emission enhancement of DHMC is distinctly specific towards Pd^{2+} (Fig. 3) as it is not affected by any other metal ions at all.

On addition of Pd^{2+} into the probe solution, the emission enhancement that occurs may be attributed to the internal charge transfer (ICT) process. When Pd^{2+} becomes coordinated to the probe, the red shift of 69 nm may take place due to this ICT mechanism. A probable binding mode of DHMC with Pd^{2+} is shown in the diagram below (Fig. 4).

There are a few reports of Pd^{2+} sensors in the literature over the years. For example, in 2019, Sinha *et al.* reported a

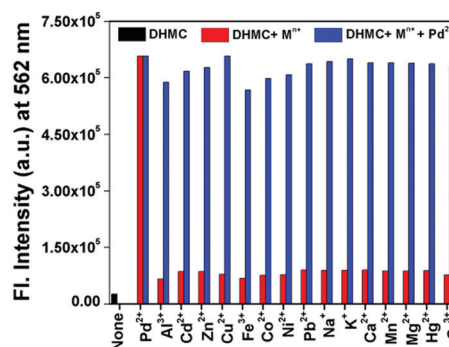


Fig. 3 Bar diagram plot of the relative emission intensity of DHMC upon addition of various metals (10 μM) in $\text{CH}_3\text{CN}/\text{H}_2\text{O}$ (4/1, v/v) (HEPES buffer, pH = 7.2) (red bars) and Pd^{2+} (20 μM) in the presence of other metal ions (blue bars).

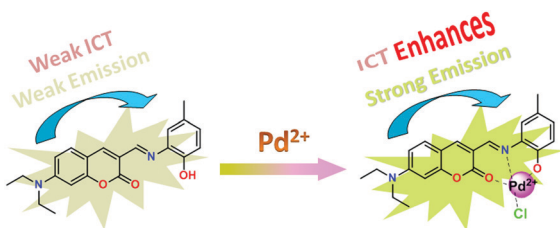


Fig. 4 Probable sensing mechanism of DHMC with Pd²⁺.

coumarinyl-rhodamine based Schiff base which detects Pd²⁺ in ethanol–water medium (8:2, v/v) with a LOD of 18.8 nM.^{14a} Then again in 2018, Qin *et al.* published an article reporting a 6-quinoxalinamine-based fluorescent probe which detects Pd²⁺ in pure water with a LOD value of 22 nM showing an “ON–OFF” emission property.^{14d} A few pyridine-2,6-dicarboxamide based sensors were synthesized in 2017 by Gupta *et al.* which showed palladium detection in HEPES buffer containing 1% DMF with detailed photophysical as well as bioimaging studies.^{14b} In 2014, Peng *et al.* reported a naphthylamine–rhodamine based ratiometric fluorescent probe to detect palladium ions in ethanol–water (1/1, v/v) with a detection limit of 49.5 nM.^{14f} In the same year, Zhu *et al.* fabricated another ratiometric probe for Pd²⁺ which was based on a cyanine moiety, displaying a LOD of 0.3 ppb.^{14g} Although these are some reports on Pd²⁺-sensors in the literature, they are not that extensively available. Further most of the organic probes were based on the rhodamine moiety and also some of them were fabricated *via* some difficult and multiple synthetic routes, which are time-consuming and sometimes cost-ineffective too. From this point of view, the fluorescent probe designed and developed herein consists of a very simple and easy synthetic pathway which is not at all time-consuming and so the Pd²⁺-detection becomes an easier experiment in this report.

pH study. The acid–base titration experiment of DHMC was carried out. From the titration, it leads to the fact that the probe DHMC shows an emission intensity enhancement in the acidic region at 562 nm, though after that the intensity drops sharply, followed by no prominent change at all further in the pH range of 5.9–10.5. But after addition of Pd²⁺ into the DHMC solution, the emission intensity increases as usual, but in the basic region it decreases sharply, thereby indicating the fact that maybe the deprotonation of the –OH group leads to this dissociation of DHMC (Fig. S12, ESI[†]). Hence the probe DHMC can be used to sense Pd²⁺ selectively in the neutral pH range with notable efficiency.

Dip-stick experiment: detection of Pd²⁺ using a TLC plate. To establish some potential application of this probe, we have carried out a popular and important experiment named the “dipstick method”, which actually suggests whether the probe can detect in the solid state too. The probe can be used as a portable fluorescent detection kit then and we can get some qualitative facts on detecting palladium in this case without the aid of any other instruments. So the experiment needs a few thin-layer chromatography (TLC) plates, which were prepared and immersed into DHMC solution (2×10^{-4} M) in acetonitrile

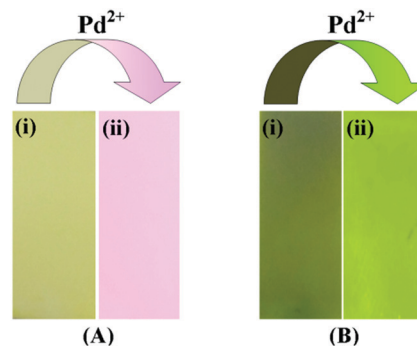


Fig. 5 Photos of TLC plates after immersion in (i) DHMC–CH₃CN solution and in (ii) DHMC–Pd²⁺–CH₃CN solution respectively under (A) ambient light and in (B) a UV chamber. [DHMC] = 2×10^{-4} M, [Pd²⁺] = 2×10^{-3} M. The excitation wavelength of the UV light is 460 nm.

and then kept for some time to evaporate the solvent. Then the TLC plates are again immersed into Pd²⁺ (2×10^{-3} M) solution and then again kept for some time to evaporate the solvent. Then after drying of both the test strips, we can notice a colour change with the naked eye. From the colour change on the TLC plates, it was observed that the colourless test strip produced green fluorescence in the presence of Pd²⁺ in a UV chamber (Fig. 5).

Crystallographic study. The structure of the probe DHMC is confirmed by the single crystal X-ray diffraction method. Detail information on the crystal analysis, data collection and structure refinement data are summarized in Table S1 (ESI[†]). The ORTEP plot with the atom numbering scheme is shown in Fig. 6.

The crystal structure of DHMC also shows strong intra-molecular and inter-molecular H-bonding and forms a 1D supramolecular chain (Fig. 7). The hydrogen atom of phenolic-OH forms bifurcated H-bonding with the imine nitrogen atom (a H1···N1 distance of 2.18(4) Å) and the O2 atom of an adjacent

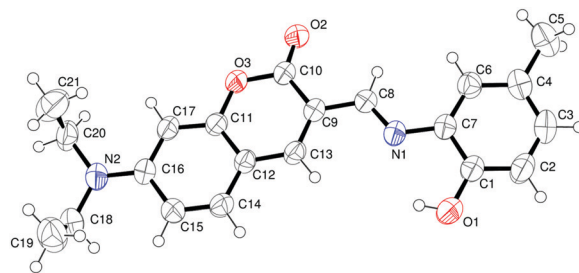


Fig. 6 ORTEP of DHMC with a 50% ellipsoidal probability (selected bond distances: O1–C1, 1.360(2) Å; O2–C10, 1.2037(19) Å; O3–C10, 1.3890(19) Å; O3–C11, 1.3759(18) Å; N1–C7, 1.408(2) Å; N1–C8, 1.267(2) Å).

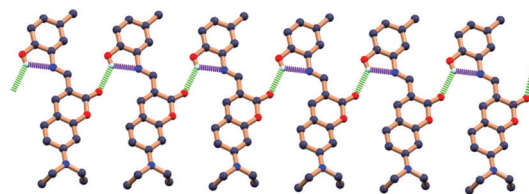


Fig. 7 1D supramolecular structure of DHMC formed by intra-molecular (●●●) and inter-molecular (●●●) H-bonding.

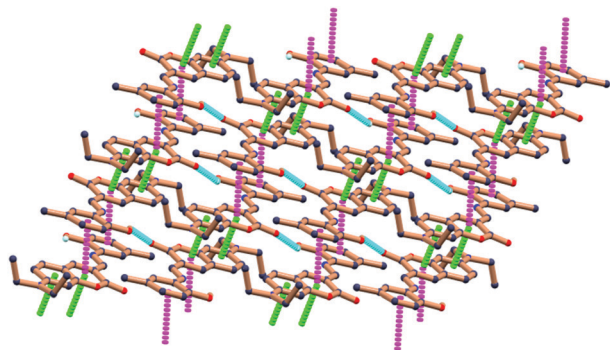


Fig. 8 2D supramolecular structure of DHMC formed by $\pi \cdots \pi$ interactions (Cg(1)···Cg(2) (●●●) and Cg(1)···Cg(2) (●●●)) and inter-molecular (●●●) H-bonding.

molecule with a H1···O2 distance of 2.35(4) Å (symmetry: $-1 + x, y, z$). Most importantly, the molecule forms a 2D-supramolecular network by $\pi \cdots \pi$ interactions and inter-molecular H-bonding (Fig. 8). Strong $\pi \cdots \pi$ interactions are present between Cg(1) and Cg(2) (symmetry: $1 - x, 2 - y, 1 - z$) and Cg(1) and Cg(3) (symmetry: $1 - x, 1 - y, 1 - z$) with Cg–Cg distances of 3.6896(10) Å and 3.6509(9) Å respectively.

Computational study. Now to gain additional information on the association between the structural changes of DHMC and its complex with Pd²⁺, we have performed density functional theory (DFT) calculations with the B3LYP/6-31+G(d) method using the Gaussian 09 program. Some selected highest occupied molecular orbitals (HOMOs) and lowest unoccupied molecular orbitals (LUMOs) of DHMC and its Pd²⁺ complex are presented in Fig. S13 and S14 (ESI[†]) respectively. Further the energy and % composition of selected molecular orbitals of DHMC–Pd²⁺ are summarised in Table S3 (ESI[†]). Now the HOMO–LUMO energy gap of DHMC is calculated to be 2.98 eV, which is notably reduced in the DHMC–Pd²⁺ complex (2.20 eV), which is also revealed by the generation of a low energy band in the complex. Then to understand the electronic transitions, time dependent density functional theory (TDDFT) was carried out on the optimized geometries of the compounds. The low energy transition for DHMC at 463 nm ($\lambda_{\text{expt.}}$, 465 nm) corresponds to the HOMO → LUMO transition. For the DHMC–Pd²⁺ complex, the low energy HOMO → LUMO transition is significantly shifted and observed at 539 nm ($\lambda_{\text{expt.}}$, 496 nm) (Table S4, ESI[†]).

Conclusions

So here we report the design and fabrication of a fluorescent “turn-on” probe which shows a distinct emission response selectively for Pd²⁺ in CH₃CN/H₂O (4/1, v/v) solvent. A significant red-shift of about 69 nm at 562 nm with a green colored fluorescence change was observed in the presence of Pd²⁺. The probe shows distinct selectivity towards Pd²⁺ over other metal cations with adequately low LOD values of the order of 7.4×10^{-8} M. The geometry of the probe is confirmed by X-ray structure analysis. The probe forms 1D and 2D supramolecular networks by strong $\pi \cdots \pi$ and inter-molecular H-bonding

interactions. The electronic structure of the probe and its probable binding modes with Pd²⁺ were thoroughly studied through DFT and TDDFT calculations too.

Conflicts of interest

There are no conflicts to declare.

Acknowledgements

The authors thank CSIR (No. 01(2992)/19/EMR-II) and SERB (No. EEQ/2018/000226), New Delhi, India for financial support. K. A. thanks the Dr D. S. Kothari fellowship for providing funding. C. K. M. thanks the RUSA 2.0 programme for a fellowship. S. G. and L. P. acknowledge UGC, New Delhi, India for providing them with fellowships.

Notes and references

- 1 S. Mukherjee, S. Chowdhury, A. K. Paul and R. Banerjee, *J. Lumin.*, 2011, **131**, 2342.
- 2 X. Chen, H. Li, L. Jin and B. Yin, *Tetrahedron Lett.*, 2014, **55**, 2537.
- 3 (a) G. Zeni and R. C. Larock, *Chem. Rev.*, 2004, **104**, 2285; (b) T. W. Lyons and M. S. Sanford, *Chem. Rev.*, 2010, **110**, 1147; (c) K. Ravindra, L. Bencs and R. V. Grieken, *Sci. Total Environ.*, 2004, **318**, 1; (d) K. Manabe, *Catalysts*, 2015, **5**, 38; (e) D. Roy and Y. Uozumi, *Adv. Synth. Catal.*, 2018, **360**, 602; (f) K. Szwaczko, O. M. Demchuk, B. Mirosław, D. Strzelecka and K. M. Pietrusiewicz, *Tetrahedron Lett.*, 2016, **57**, 3491.
- 4 T. Iwasaw, M. Tokunaga, Y. Obora and Y. Tsuji, *J. Am. Chem. Soc.*, 2004, **126**, 6554.
- 5 A. F. P. Biajoli, C. S. Schwalm, J. Limberger, T. S. Claudino and A. L. Monteiro, *J. Braz. Chem. Soc.*, 2014, **25**, 2186.
- 6 R. Jana, T. P. Pathak and M. S. Sigman, *Chem. Rev.*, 2011, **111**, 1417.
- 7 J. Kielhorn, C. Melber, D. Keller and I. Mangelsdorf, *Int. J. Hyg. Environ. Health*, 2002, **205**, 417.
- 8 L. Cui, W. Zhu, Y. Xu and X. Qian, *Anal. Chim. Acta*, 2013, **786**, 139.
- 9 (a) International Programme on Chemical Safety, Palladium, Environmental Health Criteria Series 226, World Health Organization, Geneva, 2002; (b) J. Kielhorn, C. Melber, D. Keller and I. Mangelsdorf, *Int. J. Hyg. Environ. Health*, 2002, **205**, 417; (c) C. L. Wiseman and F. Zereini, *Sci. Total Environ.*, 2009, **407**, 2493.
- 10 C. E. Garrett and K. Prasad, *Adv. Synth. Catal.*, 2004, **346**, 889.
- 11 (a) B. Dimitrova, K. Benkhedda, E. Ivanova and F. Adams, *J. Anal. At. Spectrom.*, 2004, **19**, 1394; (b) C. Locatelli, D. Melucci and G. Torsi, *Anal. Bioanal. Chem.*, 2005, **382**, 1567; (c) K. Van Meel, A. Smekens, M. Behets, P. Kazandjian and R. Van Grieken, *Anal. Chem.*, 2007, **79**, 6383.
- 12 (a) J. Yin, Y. Hu and J. Yoon, *Chem. Soc. Rev.*, 2015, **44**, 4619; (b) L. Zhu, Z. Yuan, J. T. Simmons and K. Sreenath, *RSC*

- Adv.*, 2014, **4**, 20398; (c) L. Zhu, A. H. Younes, Z. Yuan and R. J. Clark, *J. Photochem. Photobiol., A*, 2015, **311**, 1; (d) Y. Ding, Y. Tang, W. Zhu and Y. Xie, *Chem. Soc. Rev.*, 2015, **44**, 1101; (e) Z. Yuan, A. H. Younes, J. R. Allen, M. W. Davidson and L. Zhu, *J. Org. Chem.*, 2015, **80**, 5600; (f) K. P. Carter, A. M. Young and A. E. Palmer, *Chem. Rev.*, 2014, **114**, 4564; (g) K. Sreenath, Z. Yuan, J. R. Allen, M. W. Davidson and L. Zhu, *Chem. – Eur. J.*, 2015, **21**, 867.
- 13 R. Balamurugan, J.-H. Liu and B. T. Liu, *Coord. Chem. Rev.*, 2018, **376**, 196.
- 14 (a) A. K. Adak, R. Purkait, S. K. Manna, B. C. Ghosh, S. Pathak and C. Sinha, *New J. Chem.*, 2019, **43**, 3899; (b) P. Kumar, V. Kumar and R. Gupta, *RSC Adv.*, 2017, **7**, 7734; (c) A. K. Bhanja, S. Mishra, K. D. Sahab and C. Sinha, *Dalton Trans.*, 2017, **46**, 9245; (d) C. Che, X. Chen, H. Wang, J.-Q. Li, Y. Xiao, B. Fu and Z. Qin, *New J. Chem.*, 2018, **42**, 12773; (e) S. Mondal, S. K. Manna, S. Pathak, A. A. Masum and S. Mukhopadhyay, *New J. Chem.*, 2019, **43**, 3513; (f) S. Sun, B. Qiao, N. Jiang, J. Wang and X. Peng, *Org. Lett.*, 2014, **16**, 1132; (g) X. Wang, Z. Guo, S. Zhu, H. Tian and W. Zhu, *Chem. Commun.*, 2014, **50**, 13525.
- 15 M. J. Frisch, G. W. Trucks, H. B. Schlegel, G. E. Scuseria, M. A. Robb, J. R. Cheeseman, G. Scalmani, V. Barone, B. Mennucci, G. A. Petersson, H. Nakatsuji, M. Caricato, X. Li, H. P. Hratchian, A. F. Izmaylov, J. Bloino, G. Zheng, J. L. Sonnenberg, M. Hada, M. Ehara, K. Toyota, R. Fukuda, J. Hasegawa, M. Ishida, T. Nakajima, Y. Honda, O. Kitao, H. Nakai, T. Vreven, J. A. Montgomery, Jr., J. E. Peralta, F. Ogliaro, M. Bearpark, J. J. Heyd, E. Brothers, K. N. Kudin, V. N. Staroverov, R. Kobayashi, J. Normand, K. Raghavachari, A. Rendell, J. C. Burant, S. S. Iyengar, J. Tomasi, M. Cossi, N. Rega, J. M. Millam, M. Klene, J. E. Knox, J. B. Cross, V. Bakken, C. Adamo, J. Jaramillo, R. Gomperts, R. E. Stratmann, O. Yazyev, A. J. Austin, R. Cammi, C. Pomelli, J. W. Ochterski, R. L. Martin, K. Morokuma, V. G. Zakrzewski, G. A. Voth, P. Salvador, J. J. Dannenberg, S. Dapprich, A. D. Daniels, Ö. Farkas, J. B. Foresman, J. V. Ortiz, J. Cioslowski and D. J. Fox, *Gaussian 09, Revision D.01*, Gaussian, Inc., Wallingford, CT, 2009.
- 16 (a) A. D. Becke, *J. Chem. Phys.*, 1993, **98**, 5648; (b) C. Lee, W. Yang and R. G. Parr, *Phys. Rev. B: Condens. Matter Mater. Phys.*, 1988, **37**, 785.
- 17 (a) P. J. Hay and W. R. Wadt, *J. Chem. Phys.*, 1985, **82**, 270; (b) W. R. Wadt and P. J. Hay, *J. Chem. Phys.*, 1985, **82**, 284; (c) P. J. Hay and W. R. Wadt, *J. Chem. Phys.*, 1985, **82**, 299.
- 18 (a) R. Bauernschmitt and R. Ahlrichs, *Chem. Phys. Lett.*, 1996, **256**, 454; (b) R. E. Stratmann, G. E. Scuseria and M. J. Frisch, *J. Chem. Phys.*, 1998, **109**, 8218; (c) M. E. Casida, C. Jamorski, K. C. Casida and D. R. Salahub, *J. Chem. Phys.*, 1998, **108**, 4439.
- 19 (a) V. Barone and M. Cossi, *J. Phys. Chem. A*, 1998, **102**, 1995; (b) M. Cossi and V. Barone, *J. Chem. Phys.*, 2001, **115**, 4708; (c) M. Cossi, N. Rega, G. Scalmani and V. Barone, *J. Comput. Chem.*, 2003, **24**, 669.
- 20 D. Ray and P. K. Bharadwaj, *Inorg. Chem.*, 2008, **47**, 2252.